IOPscience iopscience.iop.org

Home Search Collections Journals About Contact us My IOPscience

Dynamical stabilization of the body centered cubic phase in lanthanum and thorium by phonon–phonon interaction

This article has been downloaded from IOPscience. Please scroll down to see the full text article.

2009 J. Phys.: Condens. Matter 21 175402

(http://iopscience.iop.org/0953-8984/21/17/175402)

View the table of contents for this issue, or go to the journal homepage for more

Download details:
IP Address: 129.252.86.83
The article was downloaded on 29/05/2010 at 19:27

Please note that terms and conditions apply.

J. Phys.: Condens. Matter **21** (2009) 175402 (4pp) doi:10.1088/0953-8984/21/17/175402

Dynamical stabilization of the body centered cubic phase in lanthanum and thorium by phonon–phonon interaction

P Souvatzis[1], T Björkman[2], O Eriksson[2], P Andersson[3], M I Katsnelson[4] and S P Rudin[1]

[1] Theoretical Division, Los Alamos National Laboratory, Los Alamos, NM 87545, USA
[2] Department of Physics, Uppsala University, Box 530, SE-75121, Uppsala, Sweden
[3] FOI, Swedish Defence Research Agency, SE-164 90 Stockholm, Sweden
[4] Institute for Molecules and Materials, Radboud University Nijmegen, NL-6525 ED, Nijmegen, The Netherlands

E-mail: petros.souvatzis@gmail.com

Received 30 December 2008, in final form 3 March 2009
Published 24 March 2009
Online at stacks.iop.org/JPhysCM/21/175402

Abstract
A recently developed self-consistent *ab initio* lattice dynamical method has been applied to the high temperature body centered cubic (bcc) phase of La and Th, which are dynamically unstable at low temperatures. The bcc phase of these metals is found to be stabilized by phonon–phonon interactions. The calculated high temperature phonon frequencies for La are found to be in good agreement with the corresponding experimental data.

1. Introduction

The unique physical and chemical properties of the actinides and lanthanides have attracted interest for decades. Several reviews have been written on the subject (see, e.g. [1–3]), identifying different properties which make these two series of the periodic table unique. The uniqueness stems from the progressive filling of the f shell as one traverses each series. In general one observes that the 4f-electrons in the lanthanides behave in a localized way, much in the same way they do in the atomic configurations. For the actinides (where the 5f shell becomes filled) a more complex behavior is observed: for the latter part of the series (from Am and onward) the 5f states are localized, whereas for the earlier part of the series (from Th to Np) the 5f states are itinerant and form energy bands. This becomes evident when, e.g., considering the cohesive energy and equilibrium volumes [4] as well as the structural properties [5, 6]. The element Pu sits right on the border between these parts of the actinide series, demonstrating transition from itinerant f-electrons in α-phase to the localized one in δ-phase [7, 8], and hence the electronic structure and many other properties of this material are extremely complex.

An experimental fact which is common for the lanthanides and actinides is that these elements do not usually crystallize in the body centered cubic (bcc) structure at low enough temperatures, but they melt frequently out of this structure. In this paper we have chosen to investigate this complex behavior, by studies of representative materials of the two series, i.e. La and Th. At low temperatures La and Th have the double hexagonal closed packed (dhcp) and face centered cubic (fcc) structure, respectively. The low temperature structural properties are perfectly understood from first principles theory [9, 10], showing that it is the filling of the d-band that is responsible for the structure of La [9], whereas Th is an intermediate system which has been shown to have its crystal structure governed by a balance of the occupation of the 5f and the 6d states [11]. Hence the two elements chosen in this study represent different structural and electronic properties in the ground state phases. Despite these marked differences these materials exhibit a typical behavior of the 4f and 5f series, namely that they melt out of the bcc crystal structure. It is the purpose of this report to show that the interaction between different phonon modes is responsible for the dynamical stabilization of the high temperature phase of these two series.

2. Details of the calculations

The lattice dynamical calculations of La and Th at elevated temperatures were performed using the recently

 © 2009 IOP Publishing Ltd Printed in the UK

developed self-consistent *ab initio* lattice dynamical (SCAILD) method [12]. In the SCAILD method one displaces the atoms of a supercell along several phonon modes simultaneously, in order to include the effects of phonon–phonon interactions upon the phonon frequencies at elevated temperatures. The simultaneous presence of several frozen phonons in the supercell introduces geometric disorder, i.e., entropy, which in turn renormalizes the phonon frequencies. In the SCAILD approach, the atomic displacements $\mathbf{U_R}$ of the atoms located at equilibrium Bravais lattice sites $\mathbf{R}$, are taken as superpositions of all the phonon modes s, with wavevectors $\mathbf{q}$ found to be commensurate with the cell, i.e,

$$\mathbf{U_R} = \frac{1}{\sqrt{N}} \sum_{\mathbf{q},s} \mathcal{A}_{\mathbf{q}s} \boldsymbol{\epsilon}_{\mathbf{q}s} \mathrm{e}^{\mathrm{i}\mathbf{qR}}. \tag{1}$$

Here $\boldsymbol{\epsilon}_{\mathbf{q}s}$ are the eigenvectors of the dynamical matrix

$$\mathcal{D}(\mathbf{q}) = \frac{1}{M} \sum_{\mathbf{R}} \Phi(\mathbf{R}) \mathrm{e}^{-\mathrm{i}\mathbf{qR}}, \tag{2}$$

where $\Phi(\mathbf{R})$ are the force constant matrices and

$$\mathcal{A}_{\mathbf{q}s} = \pm\sqrt{\frac{\langle \mathcal{Q}_{\mathbf{q}s} \mathcal{Q}_{-\mathbf{q}s} \rangle}{M}} = \pm\sqrt{\frac{\hbar}{M\omega_{\mathbf{q}s}} \left[\frac{1}{2} + n\left(\frac{\hbar\omega_{\mathbf{q}s}}{k_{\mathrm{B}}T}\right)\right]}, \tag{3}$$

where $n(x) = 1/(\mathrm{e}^x - 1)$ is the Planck function, M is the mass of atoms, and $\mathcal{Q}_{\mathbf{q}s}$ are the canonical phonon operators appearing together with the canonical phonon momentum, $\mathcal{P}_{\mathbf{q}s}$, in the harmonic Hamiltonian, $\mathcal{H}_h = \sum_{\mathbf{q},s} \frac{1}{2}(\mathcal{P}_{\mathbf{q}s}\mathcal{P}_{-\mathbf{q}s} + \omega^2_{\mathbf{q}s}\mathcal{Q}_{\mathbf{q}s}\mathcal{Q}_{-\mathbf{q}s})$.

The SCAILD method alternates between setting up atomic displacements based on phonon frequencies and evaluating the phonon frequencies from *ab initio* calculated forces acting on the displaced atoms. For the first iterative step, the forces stem from a direct force method calculation, see, e.g., [13, 14]. The phonon frequencies and eigenvectors corresponding to commensurate wavevectors $\mathbf{q}$, serve to calculate a set of atomic displacements $\mathbf{U_R}$ through equation (1) and (3). A first principles calculation provides the Hellman–Feynman forces acting on the displaced atoms, and a new set of phonon frequencies are obtained from the Fourier transform $\mathbf{F_q}$ of the forces,

$$\bar{\omega}_{\mathbf{q}s} = \left[\frac{\boldsymbol{\epsilon}_{\mathbf{q}s} \cdot \mathbf{F_q}}{\mathcal{A}_{\mathbf{q}s} M}\right]^{1/2}. \tag{4}$$

To clarify how the interactions between different phonon modes affect the renormalization of the phonons, we here also give the alternative expression for the new set of phonon frequencies $\bar{\omega}_{\mathbf{q}s}$ in terms of anharmonic potential coefficients [16]

$$\bar{\omega}^2_{\mathbf{q}s} = \omega^2_{\mathbf{q}s}\left(1 + \frac{\sqrt{M}}{2}\frac{\mathcal{A}_{\mathbf{q}s}}{\omega^2_{\mathbf{q}s}} \times \sum_{\mathbf{q}_1,\mathbf{q}_2}\sum_{s_1,s_2} \mathcal{R}(\mathbf{q},\mathbf{q}_1,\mathbf{q}_2,s,s_1,s_2)\frac{\mathcal{A}_{\mathbf{q}_1 s_1}\mathcal{A}_{\mathbf{q}_2 s_2}}{\mathcal{A}^2_{\mathbf{q}s}} + \cdots\right). \tag{5}$$

Here

$$\mathcal{R}(\mathbf{q},\mathbf{q}_1,\mathbf{q}_2,s,s_1,s_2) = \frac{1}{(MN)^{3/2}} \sum_{\mathbf{R},\mathbf{R}_1,\mathbf{R}_2} \sum_{\alpha,\beta,\gamma} \Phi_{\alpha\beta\gamma}(\mathbf{R},\mathbf{R}_1,\mathbf{R}_2) \times \boldsymbol{\epsilon}_{\mathbf{q}s\alpha}\boldsymbol{\epsilon}_{\mathbf{q}_1 s_1\beta}\boldsymbol{\epsilon}_{\mathbf{q}_2 s_2\gamma}\mathrm{e}^{\mathrm{i}(\mathbf{Rq}+\mathbf{R}_1\mathbf{q}_1+\mathbf{R}_2\mathbf{q}_2)}, \tag{6}$$

where $\Phi_{\alpha\beta\gamma}(\mathbf{R},\mathbf{R}_1,\mathbf{R}_2)$ are the third order coefficients appearing in the anharmonic part of the lattice dynamical Hamiltonian, see for instance [15, 16]. These coefficients describe, in terms of anharmonic changes to the nuclear potential energy, the underlying electronic structure response to the atomic displacements. Even though only third order anharmonic terms are explicitly written out in equation (5), it is now apparent that the simultaneous excitations of several commensurate phonons in the SCAILD calculation, renormalizes the phonon frequencies through anharmonic terms such as $\mathcal{R}(\mathbf{q},\mathbf{q}_1,\mathbf{q}_2,s,s_1,s_2)$. Thus these anharmonic terms can be viewed as the mediators of the phonon–phonon interaction.

The symmetry of the frequencies obtained through equation (4) is restored through

$$\Omega^2_{\mathbf{q}s} = \frac{1}{m_{\mathbf{q}}} \sum_{\mathcal{S}\in\mathcal{S}(\mathbf{q})} \bar{\omega}^2_{\mathcal{S}^{-1}\mathbf{q}s}, \tag{7}$$

where $\mathcal{S}(\mathbf{q})$ is the symmetry group of the wavevector $\mathbf{q}$ and $m_{\mathbf{q}}$ the number of elements of the group. From these symmetry restored frequencies a new set of frequencies

$$\omega^2_{\mathbf{q}s}(N_I) = \frac{1}{N_I}\sum_{i=1}^{N_I} \Omega^2_{\mathbf{q}s}(i), \tag{8}$$

are calculated. Here $\Omega_{\mathbf{q}s}(i)$, $i = 1, \ldots, N_I$ are the symmetry restored frequencies from the N_I previous iterations. The frequencies obtained through equation (8) are then used to calculate a new set of atomic displacements $\mathbf{U_R}$, through equations (1) and (3), which in turn serve to calculate a new set of forces. The iterative loop is terminated when the frequencies obtained through equation (8) have converged. For a more detailed discussion of the SCAILD method we refer the reader to the work presented in [16, 17].

From the converged commensurate phonon frequencies and their corresponding eigenvectors, the force constant matrices $\Phi(\mathbf{R})$ of La and Th were calculated by inverse Fourier transformation. The force constant matrices were then used to calculate the dynamical matrices $\mathcal{D}(\mathbf{q})$ on a mesh of 22 776 q-points in the irreducible Brillouin zone (100 × 100 × 100 Monkhorst–Pack mesh). By diagonalization of the dynamical matrices on this mesh and by applying a Gaussian smearing of 0.05 THz to each phonon frequency, the phonon density of states (DOS) was obtained for bcc-La and bcc-Th.

Regarding the details of the force calculation we used the VASP package [18], within the generalized gradient approximation (GGA). The PAW potentials used required energy cutoffs of 151 eV for La and 200 eV for Th. Monkhorst–Pack grids with a 6 × 6 × 6 mesh were used together with 0.2 eV Methfessel–Paxton smearing in all the calculations. The supercells used were all 64 atom cells, obtained by increasing the bcc primitive cell four times along the three primitive lattice vectors.

In order to get a quantitative measure of the quality of the PAW potentials used, the equilibrium lattice constants and bulk moduli were calculated and compared to their respective experimental values. Table 1 shows the results of these

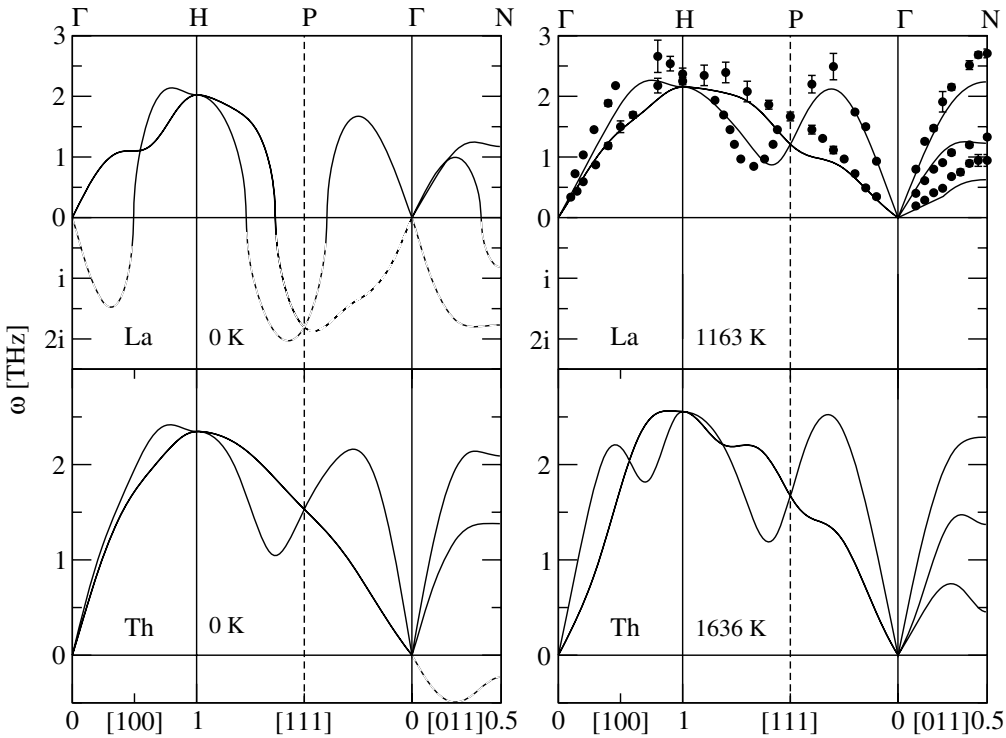

Figure 1. The right-hand panel, finite temperature SCAILD calculation of La and Th at 1163 K and 1636 K respectively. The left-hand panel, standard direct force method calculation [13] of La and Th. Here the dashed curves in the left-hand panel indicate imaginary frequencies. The filled circles and error bars are the experimental data for La of [19] measured at 1163 K.

Table 1. The zero temperature theoretical equilibrium volumes V_0 (Å^3), bulk moduli B (GPa) and pressure derivatives of the bulk moduli $B' = \partial B/\partial P$ of the metals La and Th, here presented together with experimental room temperature data. The structures corresponding to the experimental data are hcp and fcc for La and Th, respectively.

	$V_0^{(\mathrm{theor})}$	$B^{(\mathrm{theor})}$	$B'^{(\mathrm{theor})}$	$V_0^{(\mathrm{exp})}$	$B^{(\mathrm{exp})}$
La	37.3	26	2.16	37.7[a]	27.9[a]
Th	32.1	58	2.53	32.9[b]	57.7[c]

[a] Reference [21].
[b] Reference [22].
[c] Reference [23].

calculations together with experimental data. From these results no immediate doubt can be raised concerning the electronic structure part of the La and Th calculations, since calculated equilibrium properties are in a good agreement with experimental observations.

3. Results

Figure 1 shows the calculated phonon dispersions for the bcc phases of La and Th at temperatures 1163 K and 1636 K, respectively. In the case of La, the corresponding experimental data of Stassis *et al* [19] is displayed. Furthermore, we also observe that the present zero temperature calculations of La, reveal the same dynamical instabilities as in the previous work of Persson *et al* [20]. The finite temperature calculations predict the stability of the bcc phase of both La and Th by promoting the frequencies of the phonons along the Γ to N and Γ to H symmetry lines and around the P symmetry point, from imaginary to real. The finite temperature calculations of the bcc-La phonons result in an overall quantitative agreement with experimental values. Smaller deviations are observed around the H, P and N point of the Brillouin zone, most likely due to finite size effects of the supercell used in the calculations. The frequencies at commensurate wavevectors are affected by the limited cell size due to the dependence on the number of interacting phonons (the calculation only takes into account interactions between phonons with commensurate wavevectors). This differs from the direct force method, where the cell size affects the interpolation of phonon frequencies between commensurate wavevectors, but not the frequencies at commensurate wavevectors. For an example of size effects in SCAILD calculations see [17]. From equation (3) and (5) it can be seen that, at high enough temperatures, the relative shift of the squared frequency is to first order inversely proportional to the harmonic frequency: $\delta\omega^2_{\mathbf{q}s}/\omega^2_{\mathbf{q}s} \sim \omega^{-1}_{\mathbf{q}s}$. Hence the transverse phonon modes, with their generally smaller phonon frequencies (compared to the longitudinal modes) are more strongly affected by the phonon–phonon interaction.

Figure 2 shows the calculated DOS of bcc-La and bcc-Th at 1163 K and 1636 K, respectively, together with the experimental 1163 K data for La of Güthoff *et al* [19]. Here the most obvious discrepancy is that the experimental spectrum is ∼0.5 THz broader than the theoretical one. Also, compared with the theoretical DOS of La the corresponding experimental

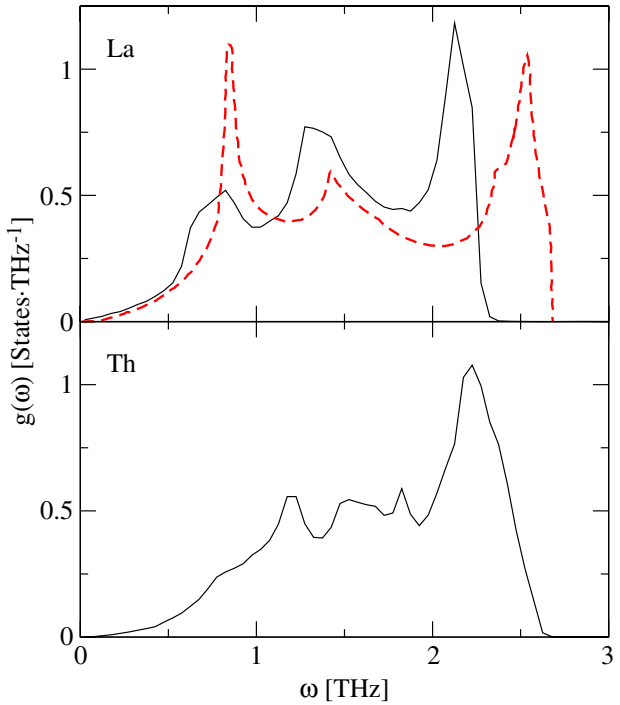

Figure 2. The phonon density of states for bcc-La and bcc-Th. The black curves are the 1163 K and 1636 K SCAILD calculations for La and Th, respectively. The dashed red line is the experimental bcc-La data calculated from the 1163 K measurements of Güthoff *et al* [19]. Both the experimental and the theoretical density of states $g(\omega)$ have been normalized so that $\int_0^\infty g(\omega)\,\mathrm{d}\omega = 1$.

(This figure is in colour only in the electronic version)

DOS has considerable more weight located at ∼0.8 THz. This lack of agreement between theory and experiment is however not surprising, since the electronic part of the bcc-La calculation has been performed without spin–orbit coupling (only scalar relativistic).

Application of the SCAILD method in the calculation to the lattice dynamical properties of the rare earths La and Th, shows that the bcc structure of these elements is dynamically stabilized by phonon–phonon interactions.

Acknowledgment

The Department of Energy supported this work under Contract No. DE-AC52-06NA25396.

References

[1] Johansson B and Li S 2007 *J. Alloys Compounds* **444** 202
[2] Wills J M and Eriksson O 2000 *Ground State Propertiess of the Actinide Elements: a Theoretical Overview, Past, Present and Future* vol 26 (Los Alamos: LA-Science) p 128
[3] See articles in Freeman A J and Lander G H (ed) 1984 *Handbook on the Physics and Chemistry of the Actinides* (Amsterdam: North-Holland)
[4] Johansson B and Rosengren A 1975 *Phys. Rev.* B **11** 1367
[5] Söderlind P, Eriksson O, Johansson B, Wills J M and Boring A M 1995 *Nature* **374** 524
[6] Söderlind P, Wills J M, Johansson B and Eriksson O 1997 *Phys. Rev.* B **55** 1997
[7] Katsnelson M I, Solovyev I V and Trefilov A V 1992 *JETP Lett.* **56** 572
[8] Savrasov S Y, Kotliar G and Abrahams E 2001 *Nature* **410** 793
[9] Skriver H L 1985 *Phys. Rev.* B **31** 1909
[10] Wills J M and Eriksson O 1992 *Phys. Rev.* B **45** 13879
[11] Johansson B, Ahuja R, Eriksson O and Wills J M 1995 *Phys. Rev. Lett.* **75** 280
[12] Souvatzis P, Eriksson O, Katsnelson M I and Rudin S P 2008 *Phys. Rev. Lett.* **100** 095901
[13] Kunc K and Martin R M 1982 *Phys. Rev. Lett.* **48** 406
[14] Souvatzis P, Delin A and Eriksson O 2006 *Phys. Rev.* B **73** 054110
[15] Wallace D C 1972 *Thermodynamic of Crystals* (New York: Dover)
[16] Souvatzis P, Eriksson O, Katsnelson M I and Rudin S P 2009 *Comput. Mater. Sci.* **44** 888–94
[17] Souvatzis P and Rudin S P 2008 *Phys. Rev.* B **78** 184304
[18] Kresse G and Furthmuller J 1996 *Phys. Rev.* B **54** 11169
[19] Güthoff F, Petry W, Stassis C, Heiming A, Hennion B, Herzig C and Trampenau J 1993 *Phys. Rev.* B **47** 2563
[20] Persson K, Ekman M and Ozoliņš V 2000 *Phys. Rev.* B **61** 11221
[21] *Chemical Rubber Company Handbook of Chemistry and Physics* 2008 89th edn (Boca Raton, FL: CRC Press)
[22] Benedict U 1987 *J. Less Common Met.* **128** 7–45
[23] Armstrong P E, Carlson O N and Smith J F 1959 *J. Appl. Phys.* **30** 36